Metamaterial-Based Two Dimensional Plasmonic Subwavelength Structures Offer the Broadest Waveband Light Harvesting

*Qiuqun Liang, Taisheng Wang, Zhenwu Lu, Qiang Sun, Yongqi Fu, and Weixing Yu**

Metamaterials, which are composed of metallic and dielectric subwavelength structures arranged in periodic array, are artificial materials with the permittivity or permeability less than that of vacuum or with negative values unattainable in nature.[1–3] Due to their unique electromagnetic properties, metamaterials have been widely used in many applications, such as sensors, superlenses, miniature antennas, and invisible cloaks.[4–7] Recently, metamaterial-based perfect absorbers have been attracted considerable attentions and various types of terahertz metamaterial absorbers have been reported. For example, Landy et al. presented a polarization-insensitive metamaterial absorber composed of metallic split ring resonators and cutting wires with singe-band absorption.[8] X.-J. He et al. proposed a dual-band metamaterial absorber made of two stacked metallic cross resonators and a lower metallic ground plane, separated by an isolation material spacer.[9] Cheng-Wen Cheng presented wide-angle polarization independent infrared dual band absorbers based on metallic multisized disk arrays.[10] Yanxia Cui proposed a sawtooth anisotropic metamaterial slab absorber for Transverse Magnetic (TM) polarized light with absorptivity higher than 95% covering a waveband ranging from 3 to 5.5 μm.[11]

However, current metamaterial absorbers suffer from many disadvantages such as narrow operating waveband, sensitivity to the polarization state of the incident light, narrow accepted angles and a fixed azimuthal angle, which greatly limit their potential applications to spectroscopic detection and phase imaging.[7–23] Hence, a light absorbing device that is broadband, wide-angle and insensitive to the incident light polarization state is urgently needed for its applications in areas mentioned above. In this letter, we propose a two-dimensional (2D) pyramidal shape metamaterial-based absorber. In comparison with previous designs, this pyramid metamaterial absorber has a very high absorptivity performance that is polarization-insensitive, wide-angle and omni-directional at full infrared waveband.

The proposed two-dimensional pyramid absorber is composed of alternating metallic and dielectric thin films as shown in the insets of **Figure 1**a. The metal thin film is made of gold with thickness t_m = 10 nm; dielectric thin film is made of germanium with thickness t_d = 190 nm. The total number of metal/dielectric pairs (*N*) is 15. These multiple thin film layers are carved into a pyramid structure for each unite cell. The periods of the unit cell in both *x* and *y* directions are 1600 nm. A gold film with a thickness (t = 100 nm) is added under the pyramid metamaterial absorber to block any incident light transmission. The optimized pyramid absorber structure was obtained through finite-difference time-domain (FDTD) simulations (Lumerical Inc.).[24] The material properties of gold and germanium were chosen from the software database- Gold Palik and Germanium Palik. Three-dimensional simulations were performed with a plane wave source incidence in *z* direction. Periodic boundary conditions were employed in both *x* and *y* directions, and a perfect matching layer boundary condition was employed in the *z* direction. The mesh size was 10 nm in both *x* and *y* directions and 5 nm in *z* direction. We used a long simulation time of 1000 fs with a step of 0.0213576 fs to ensure reliable results. We set the auto-cutoff value to 1×10^{-5} in our simulations which can be further decreased to make results even closer to the ideal cases. The frequency-dependent absorptance can be calculated by $A(\lambda) = 1 - T(\lambda) - R(\lambda)$, where the transmittance $T(\lambda) = 0$. Since a single unit cell of the absorber is a four-fold rational symmetrical pyramid structure, it has almost the same response to transverse electric (TE) polarized light and transverse magnetic polarized light for normal incidence (as is shown in Figure 1a). The absorption spectrum for normal incidence (shown in Figure 1a) indicates that the absorption performance is excellent with an absorptivity of nearly 100% at the infrared waveband from 1 μm to 14 μm. We then further studied the absorption spectra at various oblique angles for TM wave (shown in Figure 1b) and TE wave (shown in Figure 1c). In the simulations of oblique incidence cases, we employed Bloch boundary conditions in both *x* and *y* directions, while maintaining all other aforementioned parameters constant. From Figure 1b and c, one can see that the absorptivity retains up to 90% over a wide incident angle of ±60° for TM/TE polarization. Moreover, the high absorptivity of this symmetric structure almost keeps constant for any fixed

Prof. W. Yu
State Key Laboratory of Applied Optics
Changchun Institute of Optics
Fine Mechanics and Physics
Chinese Academy of Sciences
Changchun, Jilin, 130033, China
E-mail: yuwx@ciomp.ac.cn
Q. Liang
Graduate University of Chinese Academy of Sciences
Beijing, 10039, China
Dr. T. Wang, Prof. Z. Lu, Prof. Q. Sun
Opto-electronic Technology Center
Changchun Institute of Optics
Fine Mechanics and Physics
Chinese Academy of Sciences
Changchun, Jilin, 130033, China
Prof. Y. Fu
School of Physical Electronics
University of Electronic Science and Technology of China

DOI: 10.1002/adom.201200009

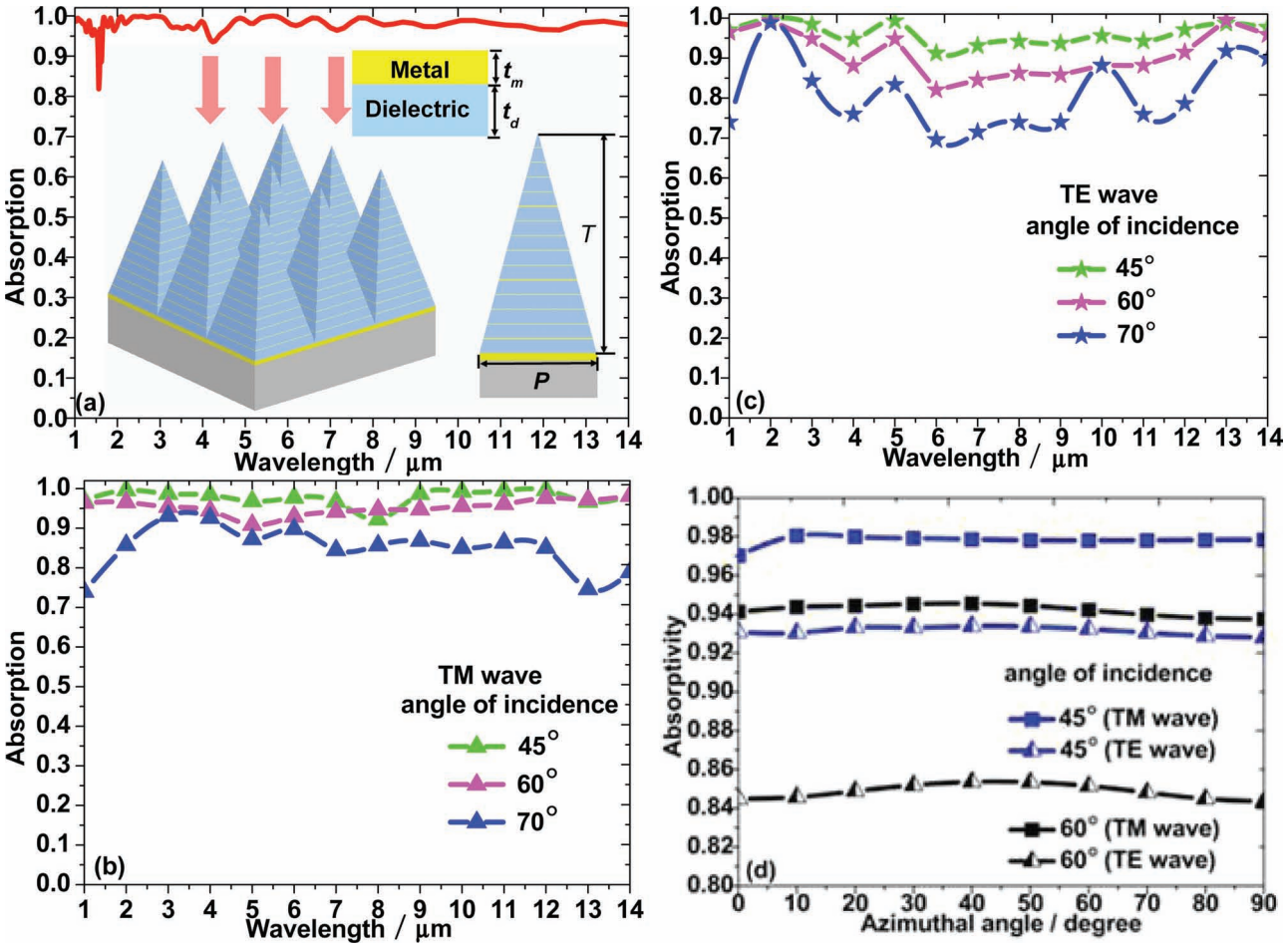

Figure 1. Absorption spectra for the multiple-layer pyramid metamaterial absorber. a) Normal incidence for TE/TM wave. b) Oblique incidence for TM wave; c) oblique incidence for TE wave, when azimuthal angle $\phi = 0$, and the oblique incident angles are $\theta = 45°$, 60°, and 70°, respectively. d) Absorptivity as a function of azimuthal angle for different incident angles, when the wavelength $\lambda_0 = 9$ μm. The insets of Figure 1(a) show the diagram of the two-dimensional subwavelength structure. $P = 1600$ nm, $T = 3000$ nm, $t_m = 10$ nm, and $t_d = 190$ nm. Number of metal/dielectric pairs $N = 15$.

incident angle θ, when the azimuthal angle increases, as demonstrated in Figure 1d for the TM and TE wave, respectively (here we choose the wavelength $\lambda_0 = 9$ μm, and the incident angles $\theta = 45°$ and 60° as examples). All these results clearly indicate that the proposed 2D metamaterial absorber has a high absorptivity performance, which is polarization-insensitive, wide-angle and omni-directional at full infrared waveband.

In order to understand the absorption mechanism of this pyramid absorber, we investigated distributions of the y-component magnetic field ($|H_y|$) and the energy flow in the plane $y = 0$ at four different wavelengths for the TM polarized incident light. The results are illustrated in **Figure 2** for $\lambda_0 =$ 3 μm, 6 μm, 9 μm, and 12 μm, respectively (owing to the symmetry design of this pyramid absorber, it's the same with TE polarization). It is found that great enhancements of the magnetic fields are excited at the specific parts of the pyramid structure from top to bottom with an increase of core width, when the incident wavelength increases. For the incident light with a shorter wavelength, such as $\lambda_0 = 3$ μm (Figure 2a), the energy is trapped at the upper part of the pyramid structure with great enhancement of the magnetic field. However, for the incident light with a longer wavelength, such as $\lambda_0 = 12$ μm (Figure 2d), the energy is trapped at the lower part of the pyramid structure with great enhancement of the magnetic field as well. These phenomena are primarily associated with the excitation of the magnetic polaritons in the dielectric layers. The magnetic polaritons in different dielectric layers couple to each other, and contribute to the resonant absorption in the structure. Consequently, the resonance in the pyramid structure can be regarded as a hybridized mode.[22,25,26] (Similar phenomenons also occur in previous reported structure depicted in Ref. 22, where the structure is made of a metallic cut-wire array positioned above a metallic film with a polymer layer in between). For various azimuthal angles, the incident plane wave can be decomposed into two components with magnetic field in x-z plane and y-z plane. Each component can effectively excite the corresponding magnetic polaritons which can greatly enhance the absorption of the energy. Meanwhile, the plots of the Poynting vectors (S) (depicted in Figure 2 by white arrows) show that, for a longer incident wavelength, the incident energy propagates downwards along z direction in the air gaps without penetrating into the structure and then whirls into the lower part of the pyramid

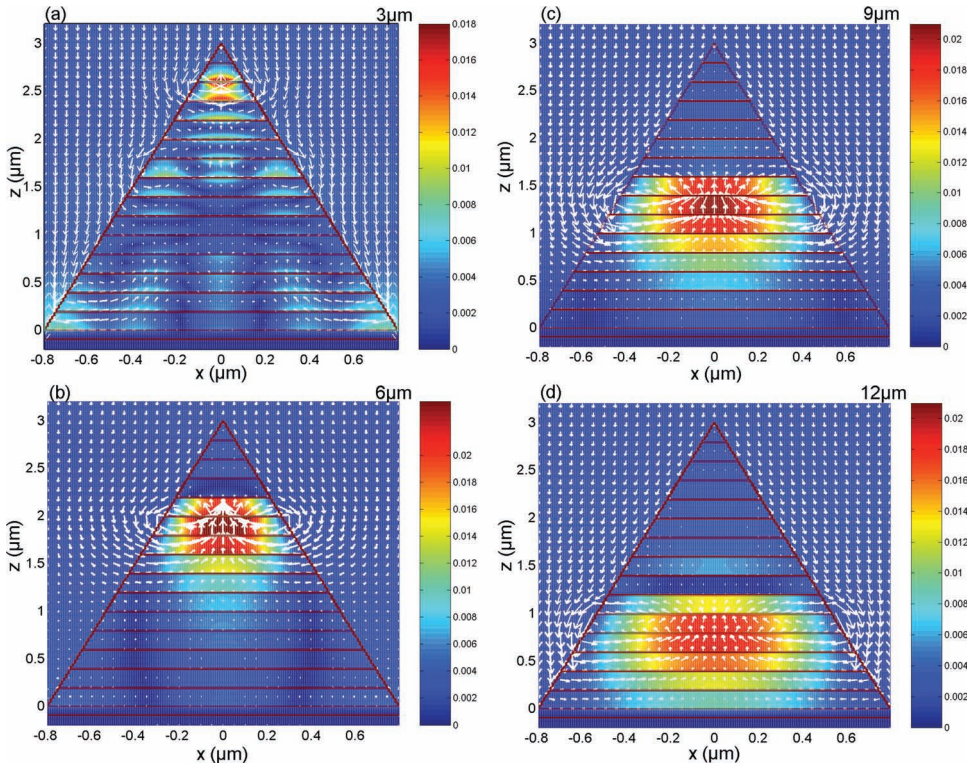

Figure 2. Distributions of the *y*-component magnetic field ($|H_y|$) (color maps) and the energy flow (arrow maps) for the pyramid metamaterial absorber at different wavelengths λ_0: (a) 3 μm, (b) 6 μm, (c) 9 μm, and (d) 12 μm, respectively. The incident wavelength for each case is shown at top right of each figure.

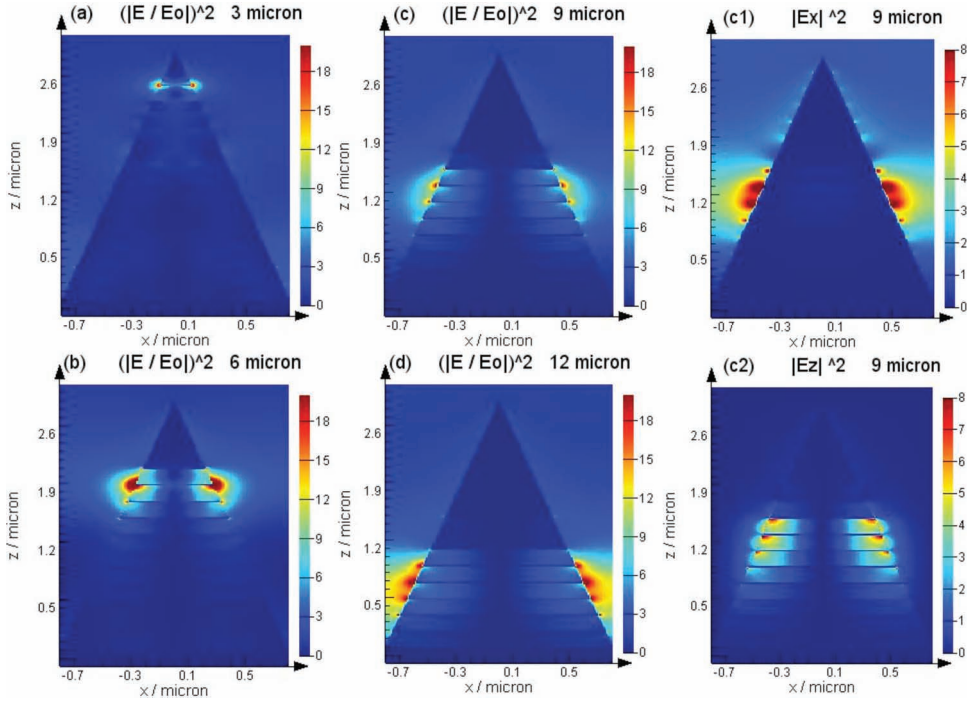

Figure 3. Distributions of the electric field ($|E/E_0|$^2) in the plane $y = 0$ at four different wavelengths λ_0: (a) 3 μm, (b) 6 μm, (c) 9 μm, and (d) 12 μm, respectively. Distributions of (c1) *x*-component of the electric field ($|E_x|$^2); (c2) *z*-component of the electric field ($|E_z|$^2) in the plane $y = 0$, when the wavelength $\lambda_0 = 9$ μm. The incident wavelength for each case is shown at the top right of each figure.

structure, which is exactly the position where the magnetic field is concentrated. These features also occur in previous sawtooth anisotropic metamaterial absorber,[11] and have already been interpreted with slow light effect in detail.[27–29] Thus, our pyramid metamaterial absorber employs the light trapping mechanism to couple and harvest light.

Moreover, due to the effects of multiple metal/dielectric thin films and the pyramidal shape, the proposed metamaterial structure can greatly suppress the reflection of light by effectively providing a graded transition of refractive index, and thus acts as an ultrabroadband multilayer antireflection coating as well.[30,31] Compared with the conventional 2D artificial dielectric (moth eye effect) made of a continuous homogeneous dielectric, which acts as an antireflection coating, our proposed pyramid absorber is made of anisotropic metamaterial with an increase of core width of metal/dielectric thin films, and thus can significantly reduce the reflection as well as greatly enhance the absorption of light over an ultrabroad spectral range. Therefore, this pyramid absorber can be regarded as a magnetic resonance light trapper to effectively absorb the inputting optical power over the broadest waveband reported ever.

To further understand the electromagnetic physics of the resonant absorption behavior, the electric field ($|E/E_0|^2$) distributions at different incident wavelengths, i.e. 3 μm, 6 μm, 9 μm, and 12 μm, were monitored computationally. As one can see from **Figure 3** that strong enhancement of the electric field

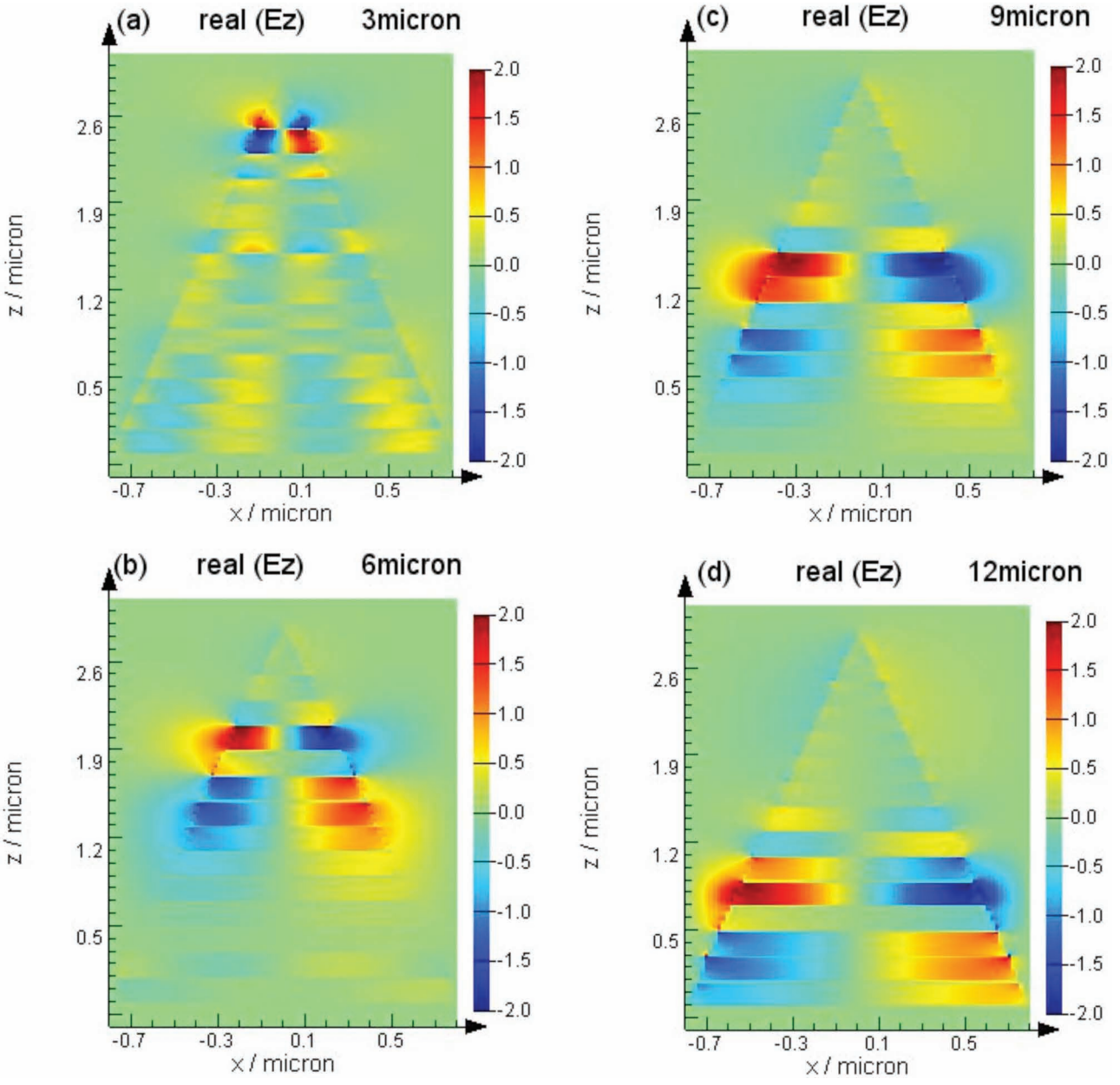

Figure 4. Distributions of the *z*-component electric field (real (E_z)) in the plane $y = 0$ at four different wavelengths λ_0: (a) 3 μm, (b) 6 μm, (c) 9 μm, and (d) 12 μm. The incident wavelength for each case is shown at top right of each figure.

has been excited at specific part of the pyramid absorber for the specific wavelength. Moreover, *x*-component of the electric field ($|E_x|^2$) is confined within the separation air gaps between neighboring unit cells (Figure 3 c1), while *z*-component of the electric field ($|E_z|^2$) is confined in the dielectric spaces (Figure 3c2). Thus, the electric field strongly concentrates at the edges of pyramid structure as well as in the air gaps between two neighboring unit cells ($|E_x|^2 > |E_z|^2$). To obtain a physical insight, the *z*-component electric field (real (E_z)) distributions in the plane $y = 0$ at four different wavelengths are illustrated in **Figure 4**. Distributions of the electric field ($|E/E_0|^2$), the *z*-component electric field (real (E_z)) and the *y*-component electric field (real (E_y)) at the metal/dielectric interface are shown in **Figure 5** (here we choose the plane $z = 1.39$ μm with wavelength $\lambda_0 = 9$ μm as an example). As shown in Figure 4, Figure 5b and c, opposite charges accumulate at the edges of the metal films, which indicates the excitation of electric dipole resonance on the metal films.[9,23] The electric dipolar resonance is due to localized surface plasmon resonance excited at the metal/dielectric interface, and therefore the local electrical field is strong enhanced.[32,33] Moreover, the electric dipoles are greatly coupled with their own images, which oscillate in anti-phase on neighboring metallic films.[22] Consequently, magnetic polaritons (or "magnetic atoms"[26,32,33]) are formed, which induce strong magnetic responses, and cause magnetic dipolar resonance between neighboring metal layers.[35] Therefore, this pyramid absorber, not only acts as an electric resonator, but also acts as a magnetic resonator. As the metal and dielectric films have different widths *w*, and thus they have different resonance frequencies. The larger the width *w* is, the smaller the resonance frequency is. By stacking the metal and dielectric layers together with the width gradually increasing, an ultrabroadband absorber with excellent absorptivity at the whole infrared waveband can be formed.

Finally, we investigated the current density (*J*) distributions to illustrate the nature of the electric and magnetic resonances. As shown in **Figure 6**, the black arrows indicate the directions of the current flow, whereas the color maps represent the current density distributions. It is apparent that, parallel and antiparallel currents are dominantly formed in the metal layers where strong enhancements of electric field and magnetic field are excited. The parallel currents result in the electric resonance.[23,34] The anti-parallel currents form a circular current and generate magnetic dipole responses, which result in the magnetic resonance in the dielectric layers.[34,36] This kind of anti-resonance is primarily due to the inhomogeneous property of the pyramid metamaterial in *z* direction and the induced strong electric-magnetic coupling.[32–38]

About the experimental verification of the ultrabroadband absorption characteristics of the proposed device, we believe that the proposed metamaterial structure could be fabricated by combining the laser interference lithography with the Ion beam etching technology. First of all, two-dimension dot arrays can be formed through two beams interference method with double exposures. Next, this two-dimensional dot arrays pattern can be transferred into the multiple thin films structure with the assistance of the Ion beam etching technology. And the pyramid structure can be achieved through adjusting the etching conditions properly.

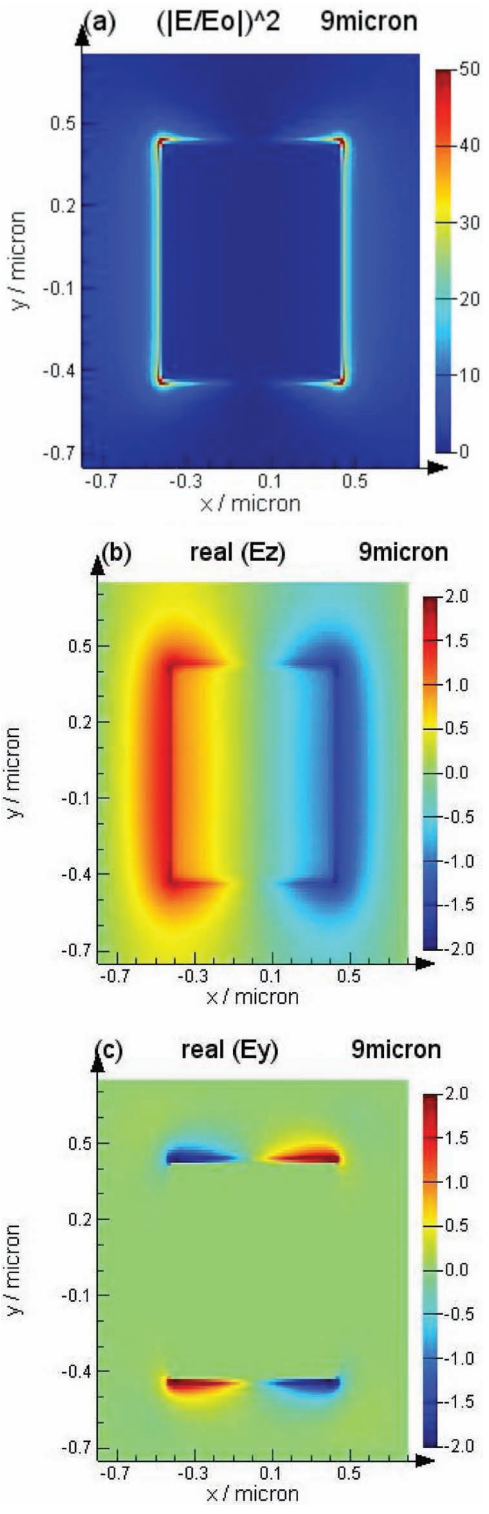

Figure 5. Distributions of (a) the electric field ($|E/E_0|^2$); (b) the *z*-component electric field (real (E_z)); c) the *y*-component electric field (real (E_y)) at the metal/dielectric interface ($z = 1.39$ μm plane), when the wavelength $\lambda_0 = 9$ μm.

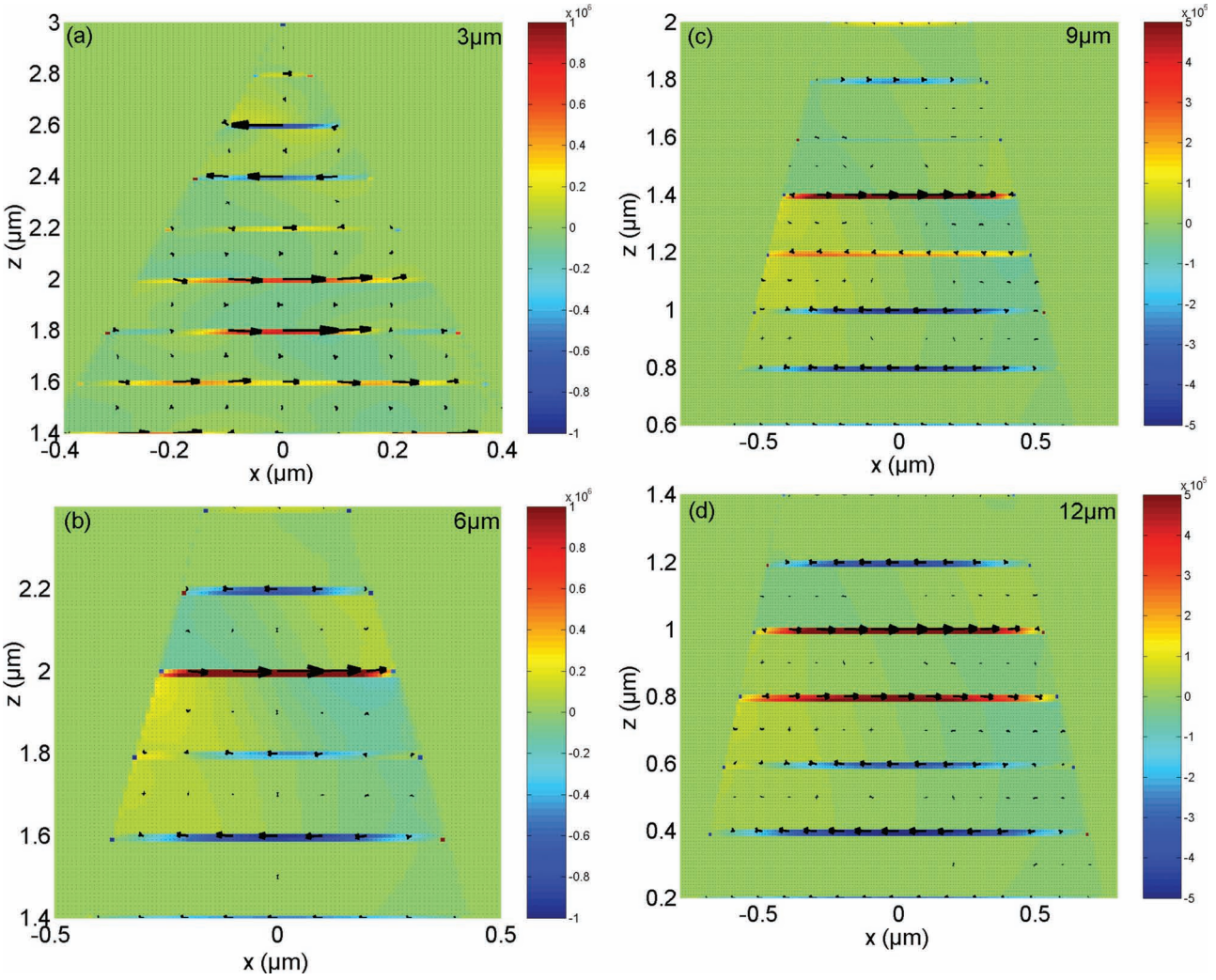

Figure 6. Current density (*J*) distributions (color maps) and current flow directions (arrow maps) in the plane $y = 0$ at four different wavelengths λ_0: (a) 3 μm, (b) 6 μm, (c) 9 μm, and (d) 12 μm. The incident wavelength for each case is shown at the top right of each figure.

In conclusion, we have proposed a two-dimensional pyramid metamaterial absorber, which performs excellently at full infrared waveband. This pyramid metamaterial absorber acts as both an electric resonator and a magnetic resonator to couple incoming electromagnetic energy into the collision of the electrons or "magnetons". By adjusting the thickness of the metal and dielectric films, the height of the pyramid structure and the period of the unit cell properly, the proposed pyramid metamaterial absorber can obtain a high absorptivity performance, not only at infrared frequencies but also at optical frequencies, microwave and terahertz frequencies.

Supporting Information

Supporting Information is available from the Wiley Online Library or from the author.

Acknowledgements

This work is supported by the National Natural Science Foundation of China with grant numbers of 90923036 and 60977041 as well as the 100 Talents Program of Chinese Academy of Sciences.

Received: September 24, 2012

[1] V. G. Sov. Veselago, *Phys. Usp.* **1968**, *10*, 509.
[2] V. M. Shalaev, *Nat. Photonics* **2007**, *1*, 41.
[3] W. Cai, V. Shalaev, *Optical Metamaterials: Fundamentals and Applications*, Springer, Singapore **2009**.
[4] N. Liu, M. Mesch, T. Weiss, M. Hentschel, H. Giessen, *Nano Lett.* **2010**, *10*, 2342.
[5] X. Zhang, Z. Liu, *Nat. Mater.* **2008**, *7*, 435.

[6] D. Dregely, R. Taubert, J. Dorfmuller, R. Vogelgesang, K. Kern, H. Giessen, *Nat. Commun.* **2011**, *2*, 267.
[7] D. Schurig, J. J. Mock, B. J. Justice, S. A. Cummer, J. B. Pendry, A. F. Starr, D. R. Smith, *Science* **2006**, *314*, 977.
[8] N. I. Landy, S. Sajuyigbe, J. J. Mock, D. R. Smith, W. J. Padilla, *Phys. Rev. Lett.* **2008**, *100*, 207402.
[9] X.-J. He, Y Wang, J.-M, Wang, T.-L, Gui, *Prog. Electromagn. Res.* **2011**, *115*, 381.
[10] C. W. Cheng, M. N. Abbas, C. W. Chiu, K. T. Lai, M. H. Shih, Y. C. Chang, *Opt. Express* **2012**, *20*, 10376.
[11] Y. Cui, J. Xu, K. H. Fung, Y. Jin, A. Kumar, S. He, X. N. Fang, *Nano Lett.* **2012**, *12*, 1443.
[12] J. Grant, Y. Ma, S. Saha, L. Lok, L. B. Lok, D. R. Cumming, *Optics Lett.* **2011**, *36*, 1524.
[13] B. Zhu, Z. Wang, C. Huang, Y. Feng, J. Zhao, T. Jiang, *Prog. Electromagn. Res.* **2010**, *101*, 231.
[14] L. Huang, H. Chen, *Prog. Electromagn. Res.* **2011**, *113*, 103.
[15] N. Liu, M. Mesch, T. Weiss, M. Hentschel, H. Giessen, *Nano Lett.* **2010**, *10*, 2342.
[16] X. L. Liu, T. Starr, A. F. Starr, W. J. Padilla, *Phys. Rev, Lett.* **2010**, *104*, 207403.
[17] J. Hendrickson, J. Guo, B. Zhang, W. Buchwald, R. Soref, *Optics Lett.* **2012**, *37*, 371.
[18] H. Tao, C. M. Bingham, D. Pilon, K. Fan, A. C. Strikwerda, D. Shrekenhamer, W. J. Padilla, X. Zhang, R. D. Averitt, *J. Phys. D: Appl. Phys.* **2010**, *43*, 225102.
[19] X. Shen, T. J. Cui, J. Zhao, H. F. Ma, W. X. Jiang, L. Hui, *Optics Lett.* **2011**, *19*, 9401.
[20] Y. Ma, Q. Chen, J. Grant, S. C. Saha, A. Khalid, D. R. S. Cumming, *Optics Lett.* **2011**, *36*, 945.
[21] D. Cheng, J. Xie, H. Zhang, C. Wang, N. Zhang, L. J. Deng, *Opt. Soc. Am. B.* **2012**, *29*, 1503.
[22] Y. Q. Ye, Y. Jin, S. L. He, *J. Opt. Soc. Am.* **2010**, *27*, 498.
[23] B. X. Zhang, Y. H. Zhao, Q. Z. Hao, B. Kiraly, I. C. Khoo, S. F. Chen, T. J. Huang, *Opt. Express* **2011**, *19*, 15221.
[24] FDTD. Lumericalhttp://www.lumerical.com/, accessed October, 2010.
[25] N. Liu, H. Guo, L. Fu, S. Kaiser, H. Schweizer, H. Giessen, *Adv. Mater.* **2007**, *19*, 3628.
[26] N. Liu, H. Guo, L. Fu, S. Kaiser, H. Schweizer, H. Giessen, *Adv. Mater.* **2008**, *19*, 3859.
[27] J. He, S. He, *IEEE Microw. Wireless Compon. Lett.* **2006**, *16*, 96.
[28] T. Jiang, J. Zhao, Y. Feng, *Opt. Express* **2009**, *17*, 170.
[29] K. L. Tsakmakidis, A. D. Boardman, O. Hess, *Nature* **2007**, *450*, 397.
[30] P. B. Clapham, M. C. Hutley, *Nature* **1973**, *244*, 281.
[31] J. Zhu, C.-M. Hsu, Z. Yu, S. Fan, Y. Cui, *Nano Lett.* **2010**, *10*, 1979.
[32] M. Pu, Q. Feng, C. Hu, X. Luo, *Plasmonics* **2012**.
[33] H. Raether, *Springer Tracts in Modern Physics,* Vol *111*, Springer, Berlin **1988**.
[34] L. Qiu, S. Wang, H. Liu, T. Li, S. Zhu, X. J. Zhang, *Opt. Soc. Am. B.* **2011**, *28*, 1655.
[35] W. Cai, U. K. Chettiar, H. K. Yuan, V. C. Silva, A. V. Kildishev, V. P. Drachev, V. M. Shalaev, *Opt. Express* **2007**, *15*, 3333.
[36] U. K. Chettiar, A. V. Kildishev, T. A. Klar, V. M. Shalaev, *Opt. Express* **2006**, *14*, 7872.
[37] Y. Ekinci1, A. Christ, M. Agio, O. J. F. Martin, H. H. Solak, J. F. Löffler, *Opt. Express* **2008**, *17*, 13287.
[38] Z. Zhang, K. Park, B. J. Lee, *Opt. Express* **2011**, *19*, 16375.